

# Layered Space-Time OFDM with High-Performance and High-Rate

Yan Xin and Georgios B. Giannakis \*

Department of ECE, University of Minnesota

200 Union Street SE, Minneapolis, MN 55455, USA

e-mails: yxin@ece.umn.edu, georgios@ece.umn.edu

## ABSTRACT

We derive a layered space-time scheme for multi-antenna orthogonal frequency-division multiplexed transmissions over frequency-selective channels. Compared with existing alternatives, the proposed scheme can attain very high spectral efficiency as well as improved performance. Enhanced diversity gains document its superior performance that is also tested by simulation.

## 1 Introduction

Deployment of multiple transmit- and receive-antennas has triggered excitement in basic and applied research, because multi-antenna communications offer the potential to improve performance and capacity of flat- [5], as well as frequency-selective fading channels [2]. When combined with orthogonal frequency division multiplexing (OFDM), multi-antenna transmissions over intersymbol interference (ISI) channels can also afford low-complexity equalization and decoding. Specific multi-antenna systems with OFDM include the Vertical Bell-labs Layered Space-Time (VBLAST) OFDM [7], and the Space-Time Coded (STC) OFDM with ST trellis or block codes [1, 3, 6]. VBLAST-OFDM is “rate-oriented” as it offers high spectral efficiency at an affordable receiver complexity, while STC-OFDM is “performance-oriented” since it is designed to maximize diversity and coding gains. However, the “jack of both trades” is not available: STC-OFDM incurs rate loss or complexity that increases with the number of transmit-antennas, while VBLAST-OFDM comes with performance loss because it neither capitalizes fully on transmit-diversity nor it exploits the multipath-diversity that becomes available with ISI channels.

It is the objective of this paper to bridge this gap, and develop a high-rate layered OFDM scheme with high-performance, and flexibility to enable desirable tradeoffs among rate, performance, and receiver complexity. We reach these goals for *frequency-selective* channels by wedging the OFDM subcarrier grouping ideas we put forth in [6], with Linear Constellation Precoding (LCP) tools [4,8], and the Diagonal (D)BLAST architecture that was originally proposed for *flat-fading* channels in [5].

*Notation:* Bold lower (upper) case fonts will be used to denote column vectors (matrices);  $(\cdot)^T$ ,  $(\cdot)^H$ , and  $[\cdot]_{ij}$ , will represent transpose, Hermitian, and the  $(i, j)$ th entry of a matrix, respectively.

## 2 Precoding, DBLAST, and OFDM

Consider a multi-antenna system with  $N_t$  transmit- and  $N_r$  receive-antennas, where OFDM transmissions with  $N_c$  carriers are employed as depicted in Fig. 1. The fading channel between the  $m$ th transmit- and the  $n$ th receive-antenna is frequency-selective with discrete-time baseband equivalent finite impulse response (FIR) coefficients collected in the  $(L + 1) \times 1$  vector  $\mathbf{h}_{nm} \triangleq [h_{nm}(0), \dots, h_{nm}(L)]^T$ , with  $m = 1, \dots, N_t$ , and  $n = 1, \dots, N_r$ . We assume that:

- (as) the  $N_t(L + 1) \times 1$  channel vector  $\mathbf{h}_n \triangleq [\mathbf{h}_{1n}^T, \dots, \mathbf{h}_{N_t n}^T]^T$  is zero-mean, complex Gaussian, with full rank correlation matrix  $\mathbf{R}_h \triangleq E(\mathbf{h}_n \mathbf{h}_n^H)$ . However,  $\mathbf{h}_n$ 's for different  $n$  are statistically independent, which can be satisfied by well separating the  $N_r$  receive-antennas.

Notice that we allow for correlated wireless channels with e.g., an exponential power delay profile.

The information symbol stream  $\{s_i\}$  is first demultiplexed to  $N_t$  sub-streams,  $\{s_{i,m}\}_{m=1}^{N_t}$ , one for each transmit-antenna. Every sub-stream, say the  $m$ th, is parsed into blocks, each containing  $N_c$  symbols, as many as the system carriers. We select  $N_c = N_g(L + 1)$ , and split every block of  $N_c$  symbols into  $N_g$  groups, each containing  $L + 1$  symbols. Let  $\mathbf{s}_m^{(p)}$  denote the  $p$ th  $N_c \times 1$  such block of the  $m$ th sub-stream. The  $g$ th group from this block is denoted by  $\mathbf{s}_{g,m}^{(p)}$ , and is particularly chosen to contain the  $L + 1$  symbols  $\{s_{lN_g + g, m}^{(p)}\}_{l=0}^L$ . Forming likewise all  $N_g$  groups will turn out to reduce decoding complexity, but as we will see later, when this particular grouping is combined with precoding, it will also enable the maximum diversity gains (see also [6]).

Collecting  $\mathbf{s}_{g,m}^{(p)}$  blocks across all  $N_t$  antennas, we form the  $N_t(L + 1) \times 1$  vector  $\mathbf{s}_g^{(p)} \triangleq [\mathbf{s}_{g,1}^{(p)T}, \dots, \mathbf{s}_{g,N_t}^{(p)T}]^T$  on which we apply linear constellation precoding (LCP) to obtain  $\Theta \mathbf{s}_g^{(p)}$ , where  $\Theta$  is the  $N_t(L + 1) \times N_t(L + 1)$  LCP matrix. With reference to Fig. 1, and  $\boldsymbol{\theta}_{lN_t + m}^T$  denoting the  $(lN_t + m)$ th

\*This work was supported by the NSF Wireless Initiative grant no. 99-79443, and by the ARL/CTA grant no. DAAD19-01-2-011.

row of  $\Theta$ , the  $(lN_t + m)$ th entry,  $\theta_{lN_t+m}^T \mathbf{s}_g^{(p)}$ , of the  $p$ th precoded block will form the  $l$ th symbol with  $l = 0, \dots, L$  in the  $g$ th group of the  $m$ th LCP mapper output. Repeating this for all  $N_g$  groups of  $L + 1$  symbols, describes how the  $N_t$  input blocks indexed by  $p$  (containing  $N_c$  symbols each) are mapped via LCP to yield  $N_t$  output blocks that are also indexed by  $p$ , and each contains  $N_c$  symbols. Notice that each output symbol is formed as a linear combination of  $N_t(L + 1)$  symbols from *all*  $N_t$  input sub-streams. This is precisely what enables  $\Theta$  to collect both transmit- as well as multipath-diversity gains.

Consider now a collection of  $N_l$  input blocks  $\{\mathbf{s}_m^{(p)}\}_{p=1}^{N_l}$  per sub-stream, and the corresponding LCP output blocks, each organized in  $N_g$  groups as before:  $\{\Theta \mathbf{s}_g^{(p)}, g = 1, \dots, N_g\}_{p=1}^{N_l}$ . With the latter as  $N_t$ -branch input, the DBLAST module depicted in Fig. 1 outputs a set of  $N_t \times N$  matrices  $\{\mathbf{C}_g(l), g = 1, \dots, N_g, l = 0, \dots, L\}$ , defined as:

$$\mathbf{C}_g(l) \triangleq \begin{bmatrix} c_{g,1}^{(1)}(l) & \cdots & c_{g,1}^{(N_l)}(l) & 0 & \cdots & 0 \\ 0 & c_{g,2}^{(1)}(l) & \cdots & c_{g,2}^{(N_l)}(l) & \ddots & 0 \\ \vdots & \ddots & \ddots & \cdots & \ddots & 0 \\ 0 & \cdots & 0 & c_{g,N_t}^{(1)}(l) & \cdots & c_{g,N_t}^{(N_l)}(l) \end{bmatrix} \quad (1)$$

where the number of columns  $N = N_l + N_t - 1$ , and  $[\mathbf{C}_g(l)]_{mq} \triangleq c_{g,m}^{(p)}(l) \triangleq \theta_{lN_t+m}^T \mathbf{s}_g^{(p)}$ , with  $p = q - m + 1$ ,  $q \in [m, N_l + m - 1]$ , and “0” otherwise. Notice that  $\mathbf{C}_g(l)$  is structurally reminiscent of the DBLAST code matrix with  $N_l$  layers (diagonals) [5]. Since  $l \in [0, L]$  and  $g \in [1, N_g]$ , we can use  $k = lN_g + g$  to index the  $N_c$  LCP-mapper output symbols per block, and re-label each entry  $[\mathbf{C}_g(l)]_{mq}$  as  $[\mathbf{C}(k)]_{mq}$ .

We then feed  $\mathbf{c}_{mq} \triangleq [[\mathbf{C}(1)]_{mq}, \dots, [\mathbf{C}(N_g)]_{mq}]^T$  as input to the inverse fast Fourier transform (IFFT) processor of the  $m$ th antenna during the  $q$ th block (OFDM block-symbol). Next, we take the  $N_c$ -point IFFT to obtain  $\tilde{\mathbf{c}}_{mq} = \text{IFFT}[\mathbf{c}_{mq}]$ , where  $[\tilde{\mathbf{c}}_{mq}]_k$  denotes the  $k$ th entry of  $\tilde{\mathbf{c}}_{mq}$ . Prepending the cyclic prefix (CP) of length  $L$ , we obtain for each  $(m, q)$  an  $(N_c + L) \times 1$  block  $\bar{\mathbf{c}}_{m,q}$  with entries  $\{[\tilde{\mathbf{c}}_{mq}]_{N_c-L+1} \cdots [\tilde{\mathbf{c}}_{mq}]_{N_c} [\tilde{\mathbf{c}}_{mq}]_1 \cdots [\tilde{\mathbf{c}}_{mq}]_{N_c}\}$ , that we subsequently digital-to-analog convert, pulse shape, and transmit from the  $m$ th antenna during the  $q$ th block. Our transmitted  $N_t \times N(N_c + L)$  space-time code matrix is:

$$\bar{\mathbf{C}} \triangleq \begin{bmatrix} \bar{\mathbf{c}}_{1,1}^T & \bar{\mathbf{c}}_{1,2}^T & \cdots & \bar{\mathbf{c}}_{1,N_t}^T & \mathbf{0}^T & \cdots & \mathbf{0}^T \\ \mathbf{0}^T & \bar{\mathbf{c}}_{2,1}^T & \bar{\mathbf{c}}_{2,2}^T & \cdots & \bar{\mathbf{c}}_{2,N_t}^T & \ddots & \vdots \\ \vdots & \ddots & \ddots & \ddots & \cdots & \ddots & \mathbf{0}^T \\ \mathbf{0}^T & \cdots & \mathbf{0}^T & \bar{\mathbf{c}}_{N_t,1}^T & \bar{\mathbf{c}}_{N_t,2}^T & \cdots & \bar{\mathbf{c}}_{N_t,N_t}^T \end{bmatrix}. \quad (2)$$

All the FIR channels are supposed to remain invariant over  $N(N_c + L)$  symbol periods. The number of nonzero block entries  $\bar{\mathbf{c}}_{mq}^T$  in  $\bar{\mathbf{C}}$  is  $N_l N_t = (N - N_t + 1)N_t$ ; and each  $1 \times (N_c + L)$  block entry  $\bar{\mathbf{c}}_{mq}^T$  carries  $N_c$  information symbols (since  $L$  redundant symbols correspond to the CP). With these symbols drawn from the alphabet of size  $|\mathcal{A}_s|$ , our

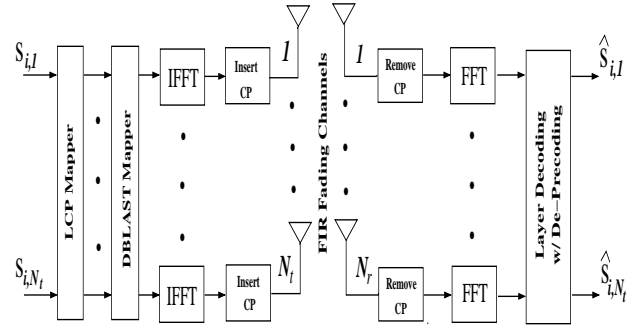


Figure 1: System model

transmission rate is found to be:

$$R = \frac{N_t(N - N_t + 1)N_c \log_2 |\mathcal{A}_s|}{N(N_c + L)} \text{ bps/Hz.}$$

Clearly, selecting  $N \gg N_t$  and  $N_c \gg L$  leads to very high rates relative to the STC-OFDM in [1, 3, 6]. To appreciate the flexibility and improved performance of our scheme over the high-rate VBLAST-OFDM in [7], we turn to the receiver and consider the input-output relationship per carrier.

We suppose that carrier synchronization, channel acquisition, timing, and symbol-rate sampling have been accomplished successfully at the receiver. We then remove the CP, and subsequently take the  $N_c$ -point FFT of each block at the output of each antenna's receive-filter. Recall that the CP insertion and removal along with the IFFT and FFT taken at the transmitters and receivers, respectively, convert the  $N_t N_r$  frequency selective channels to a set of  $N_t N_r N_c$  flat fading sub-channels. Specifically, the samples of the  $q$ th block at the  $n$ th receive-filter output obey the following input-output relationship on the  $k$ th carrier:

$$y_{nq}(k) = \sum_{m=1}^{N_t} H_{nm}(k) [\mathbf{C}(k)]_{mq} + w_{nq}(k), \quad (3)$$

where  $H_{nm}(k)$  is the frequency response of  $\mathbf{h}_{nm}$  at the  $k$ th carrier, i.e.,  $H_{nm}(k) = \sum_{l=0}^L h_{nm}(l) e^{-j2\pi lk/N_c}$ , and  $w_{nq}(k)$ 's are independent complex Gaussian random variables with zero mean and variance  $N_0$ .

Collecting samples  $y_{nq}(k)$  from all  $N_r$  receive-antennas, and across all  $N$  blocks (OFDM block-symbols), for a fixed carrier  $k$ , we can recast (3) in a compact matrix form:  $\mathbf{Y}(k) = \mathbf{H}(k)\mathbf{C}(k) + \mathbf{W}(k)$ , where  $[\mathbf{Y}(k)]_{nq} \triangleq y_{nq}(k)$ ,  $[\mathbf{H}(k)]_{nm} \triangleq H_{nm}(k)$ , and  $[\mathbf{W}(k)]_{nq} \triangleq w_{nq}(k)$ . Re-writing  $k$  as  $k = lN_g + g$ , we will pursue decoding per group  $g$ , in which the following relationship holds:

$$\mathbf{Y}_g(l) = \mathbf{H}_g(l)\mathbf{C}_g(l) + \mathbf{W}_g(l), \quad (4)$$

where  $\mathbf{Y}_g(l) \triangleq \mathbf{Y}(lN_g + g)$ ,  $\mathbf{H}_g(l) \triangleq \mathbf{H}(lN_g + g)$ ,  $\mathbf{C}_g(l) \triangleq \mathbf{C}(lN_g + g)$ , and  $\mathbf{W}_g(l) \triangleq \mathbf{W}(lN_g + g)$ .

In a nutshell, we have developed a layered space time system, which can be viewed as a block version of DBLAST that is combined with OFDM to enable high-rate multi-antenna

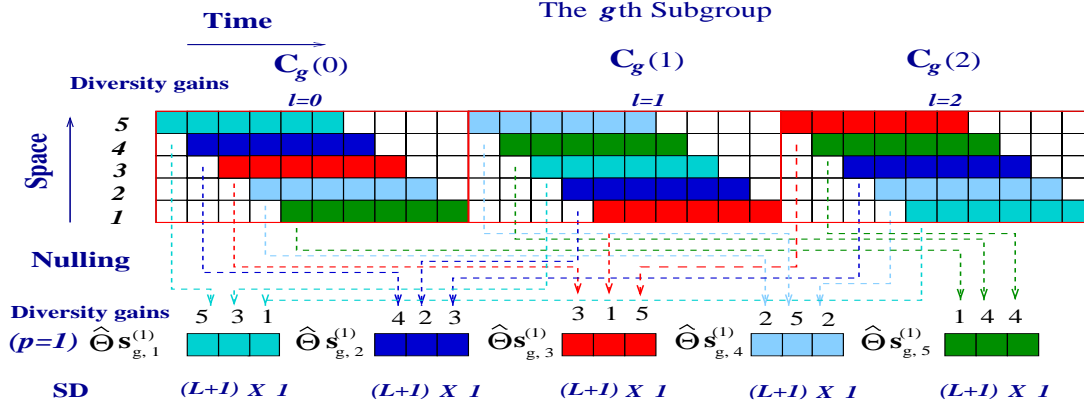


Figure 2: An encoding/decoding example of option 2

transmissions over frequency selective channels. As the term DBLAST-OFDM-LCP indicates, our scheme relies also on linear constellation precoding. As we will see next, LCP applied to groups of carriers enriches our high-rate OFDM with multipath diversity at an affordable receiver complexity.

### 3 Decoding and Performance

Recall from (1) that  $[\mathbf{C}_g(l)]_{mq} \triangleq \boldsymbol{\theta}_{lN_t+m}^T \mathbf{s}_g^{(q-m+1)}$ . We can see that the information symbols in  $\mathbf{s}_g \triangleq [\mathbf{s}_g^{(1)T} \dots \mathbf{s}_g^{(N_t)T}]^T$  are spread across all the carriers of group  $g$ . Thus, we need to consider  $\mathbf{C}_g \triangleq [\mathbf{C}_g(0) \dots \mathbf{C}_g(L)]$  when decoding  $\mathbf{s}_g$ . Maximum-likelihood (ML) decoding can then be performed per group of carriers to yield:  $\hat{\mathbf{s}}_g = \arg \min_{\mathbf{s}_g} \sum_{l=0}^L \|\mathbf{Y}_g(l) - \mathbf{H}_g(l)\mathbf{C}_g(l)\|^2$ . Albeit computationally heavy, when  $\Theta$  is properly designed and  $N \geq N_t$ , ML decoding enables the maximum possible diversity order  $N_t N_r (L+1)$  [9]. This benchmarks the performance of sub-optimal but practical decoders that have lower complexity than ML. Those require  $N_r \geq N_t$ , and rely on the null-and-cancel decoding [5].

The corresponding algorithm starts with the  $N_r \times N_t$  par-unitary matrix  $\mathbf{Q}_g(l)$  in the QR factorization of  $\mathbf{H}_g(l) = \mathbf{Q}_g(l)\mathbf{U}_g(l)$ , and uses  $\mathbf{Q}_g(l)$  in (4) to form the matrix  $\bar{\mathbf{R}}_g(l) \triangleq \mathbf{Q}_g^H(l)\mathbf{Y}_g(l) = \mathbf{U}_g(l)\mathbf{C}_g(l) + \mathbf{Q}_g^H(l)\mathbf{W}_g(l)$ , where  $\mathbf{U}_g(l)$  is an  $N_t \times N_t$  upper triangular matrix. Suppose we have decoded the first  $(p-1)$  layers that correspond to the first  $(p-1)$  diagonals in (1). To decode the block  $\mathbf{s}_g^{(p)}$ , we consider the  $(m, p+m-1)$  entry of  $\bar{\mathbf{R}}_g(l)$  that can be written as  $\bar{r}_{g,m}^{(p)}(l) = U_{g,m}(l)\boldsymbol{\theta}_{lN_t+m}^T \mathbf{s}_g^{(p)} + \mathcal{L}(\mathbf{s}_g^{(1)}, \dots, \mathbf{s}_g^{(p-1)}) + v_{g,m}^{(p)}(l)$ , where  $\mathcal{L}(\mathbf{s}_g^{(1)}, \dots, \mathbf{s}_g^{(p-1)})$  contains symbols from previously decoded layers, and  $v_{g,m}^{(p)}(l)$  denotes the  $(m, m+p-1)$ th entry of  $\mathbf{Q}_g^H(l)\mathbf{W}_g(l)$ . If all previous layers have been decoded correctly, we can cancel the term  $\mathcal{L}(\mathbf{s}_g^{(1)}, \dots, \mathbf{s}_g^{(p-1)})$  to obtain

$$r_{g,m}^{(p)}(l) = U_{g,m}(l)\boldsymbol{\theta}_{lN_t+m}^T \mathbf{s}_g^{(p)} + v_{g,m}^{(p)}(l). \quad (5)$$

What boosts performance of the nulling-cancelling iteration in our case is the “de-precoding” step that is needed after the interference nulling to decode  $\mathbf{s}_g^{(p)}$

from the LCP blocks  $\boldsymbol{\theta}_{lN_t+m}^T \mathbf{s}_g^{(p)}$  in (5). Collecting eq. (5) for  $l = 0, \dots, L$  and  $m = 1, \dots, N_t$ , we perform de-precoding per layer  $p$  of each group  $g$ , based on the block:  $\mathbf{r}_g^{(p)} = \mathbf{D}_g^{(p)}\Theta \mathbf{s}_g^{(p)} + \mathbf{v}_g^{(p)}$ , where  $\mathbf{v}_g^{(p)} \triangleq [v_{g,1}^{(p)}(0) \dots v_{g,N_t}^{(p)}(0) \dots v_{g,1}^{(p)}(L) \dots v_{g,N_t}^{(p)}(L)]^T$ ,  $\mathbf{D}_g^{(p)} \triangleq \text{diag}[U_{g,1}(0) \dots U_{g,N_t}(0) \dots U_{g,1}(L) \dots U_{g,N_t}(L)]$ , and  $p = 1, \dots, N_t$ . This step is implemented using the Sphere-Decoding (SD) algorithm that is known to exhibit near-ML performance at complexity that is  $\mathcal{O}[(N_t(L+1))^6]$  [4]. Even lower complexity de-precoding is possible by inverting  $\Theta \mathbf{s}_g^{(p)}$  in the zero-forcing or minimum mean-square sense (see [6, 8] for details).

We prove in [9] that under proper conditions on the channel and the precoder, the diversity order with layer decoding (that includes de-precoding) is:  $G_d^{(p)} = [N_r N_t - (N_t - 1)N_t/2](L+1)$ , regardless of the layer  $p = 1, \dots, N_t$ . This is in agreement with the original DBLAST scheme applied to flat-fading channels, where the layer decoding order does not affect performance when one assumes that previous layers have been decoded correctly. The  $\Theta$ 's satisfying our conditions in [9] are those we have constructed in [8, eq. (7)].

### 4 Reduced-complexity encoding/decoding options

In order to enable large joint transmit- and multipath-diversity gains, our scheme uses the precoder  $\Theta$  of size  $N_t(L+1)$ , which leads to very high decoding complexity when  $N_t(L+1)$  is large. To reduce the decoding complexity, we propose the following two reduced-complexity encoding/decoding options.

*Option 1:* If instead of  $L+1$  symbols, only one symbol is taken per sub-stream as input to the LCP mapper, then  $\mathbf{s}_{g,m}^{(p)}$  reduces to a scalar (call it  $s_{n_c,m}^{(p)}$  with  $n_c = 1, \dots, N_c$ ). The LCP matrix (call it  $\hat{\Theta}$ ) becomes  $N_t \times N_t$ , and each LCP output symbol is now a linear combination of  $N_t$  input symbols. Because  $\hat{\Theta}$  is smaller than  $\Theta$ , this leads to reduced complexity de-precoding, but ensures only full transmit-diversity gain.

*Option 2:* Instead of using one  $N_t(L+1) \times N_t(L+1)$  precoder  $\Theta$  for all  $N_t$  sub-streams, we can use  $N_t$  precoders of size  $L+1$  with each one (call it  $\hat{\Theta}$ ) for each sub-stream.

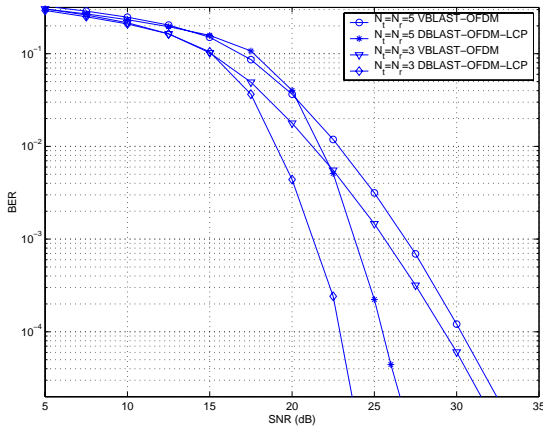


Figure 3: DBLAST-OFDM-LCP vs. VBLAST-OFDM

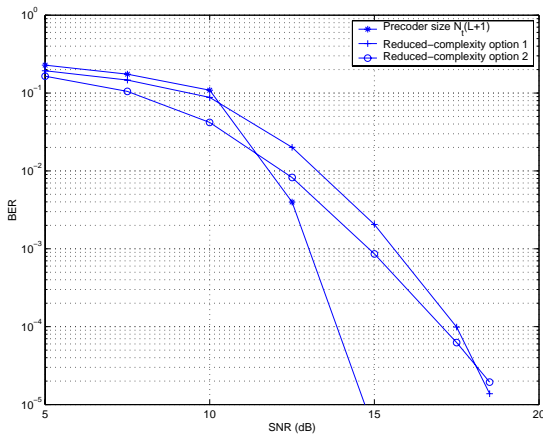


Figure 4: DBLAST-OFDM-LCP encoding/decoding options

Thus, each  $\hat{\Theta}\mathbf{s}_{g,m}^{(p)}$  is a  $(L+1) \times 1$  precoded block, and each LCP output symbol is now a linear combination of  $L+1$  input symbols. The  $N_t$  precoded blocks  $\{\hat{\Theta}\mathbf{s}_{g,m}^{(p)}\}_{m=1}^{N_t}$  of the LCP mapper output pass through the DBLAST mapper, which maps  $\{\hat{\Theta}\mathbf{s}_{g,m}^{(p)}\}_{m=1}^{N_t}$  ( $p = 1, \dots, N_t$ ) to  $\mathbf{C}_g(l)$ 's ( $l = 0, \dots, L$ ) so that each precoded block  $\hat{\Theta}\mathbf{s}_{g,m}^{(p)}$  has the same (or almost same) diversity gains (see [9] for details). Because the size of  $\hat{\Theta}$  is much smaller than  $\Theta$ , this reduces the de-precoding complexity considerably. Also notice that the diversity gain of each entry in a diagonal layer is different. By suitably designing the DBLAST mapper, we can still achieve very high diversity gains. Specifically, it is shown in [9] that when either  $L$  or  $N_t$  is odd, a diversity gain  $(N_t+1)(L+1)/2$  can be achieved for each precoded block. For example, in the case of  $N_t = N_r = 5$  and  $L = 2$ , the diversity gain of the  $i$ th entry ( $i = 1, \dots, 5$ ) in a diagonal layer is  $N_t - i + 1$ . Fig. 2 shows that each  $(L+1) \times 1$  precoded vector can achieve diversity gain nine when a carefully designed DBLAST mapper is used.

Fig. 3 depicts a performance comparison between DBLAST-OFDM-LCP and VBLAST-OFDM. Using  $N_c = 15$  and  $L = 2$ , we test two cases for  $N_t = N_r = 5$ , and  $N_t = N_r = 3$  with 16-QAM. We use Reed-Solomon (15,9)

codes for VBLAST-OFDM, and the precoder  $\Theta$  of [8, eq. (7)] for DBLAST-OFDM-LCP. Since the transmit-diversity order is high for  $N_t = N_r = 5$ , we apply option 1 to reduce the complexity at the expense of multipath-diversity loss (see discussion before (1)). To ensure identical transmission rates for VBLAST-OFDM and DBLAST-OFDM-LCP, we choose  $N = 5$  when  $N_t = N_r = 3$ , and  $N = 10$ , when  $N_t = N_r = 5$ . The corresponding rates are  $R = 6.35$  bps/Hz, and  $R = 10.58$  bps/Hz, respectively. Fig. 3 corroborates that DBLAST-OFDM-LCP outperforms VBLAST-OFDM considerably (about 5 dB at  $\text{BER} = 10^{-4}$ ). Choosing  $N_c = 15$ ,  $N_t = N_r = 5$ , and QPSK, we compare the performance between different encoding/decoding options for  $L = 2$  in Fig. 4. The encoding/decoding scheme using the precoder of size  $N_t(L+1) \times N_t(L+1)$  outperforms two reduced-complexity options considerably at the expense of much higher decoding complexity. Interestingly, option 2 outperforms option 1 for SNR values up to 18 dB even though it has lower complexity than option 1. This is due to the fact that option 2 has a larger coding gain than option 1, while option 1 has a larger diversity gain than option 2.

## References

- [1] D. Agrawal, V. Tarokh, A. Naguib, and N. Seshadri, "Space-time coded OFDM for high data-rate communication over wideband channels," in *Proc. Vehicular Technology Conf.*, Ottawa, ON, Canada, May 18-21, 1998, pp. 2232-2236.
- [2] S. L. Ariyavisitakul, "Turbo space-time processing to improve wireless channel capacity," *IEEE Trans. on Comm.*, vol. 48, no. 8, pp. 1347-1359, Aug. 2000.
- [3] R. S. Blum, Y. Li, J. H. Winters, and Q. Yan, "Improved space-time coding for MIMO-OFDM wireless communications," *IEEE Trans. on Comm.*, vol. 49, no. 11, pp. 1873-1878, Nov. 2001.
- [4] J. Boutros and E. Viterbo, "Signal space diversity: A power and bandwidth efficient diversity technique for the Rayleigh fading channel," *IEEE Trans. on Info. Theory*, vol. 44, no.4, pp. 1453-1467, July 1998.
- [5] G. J. Foschini and M. J. Gans, "Layered space-time architecture for wireless communication in a fading environment when using multiple antennas," *Bell Labs. Syst. Tech. J.*, vol. 1, pp. 41-59, Autumn 1996.
- [6] Z. Liu, Y. Xin, and G. B. Giannakis, "Space-Time-Frequency Coded OFDM over Frequency-Selective Fading Channels," *IEEE Transactions on Signal Processing*, Oct., 2002. also in *Proc. of Intl. Conf. on ASSP*, Orlando, FL, May 13-17, 2002. downloadable from <http://spincom.ece.umn.edu/xin/STF.pdf>.
- [7] R. J. Piechocki, P. N. Fletcher, A. R. Nix, C. N. Canagarajah, and J. P. McGeehan, "Performance evaluation of BLAST-OFDM enhanced Hiperlan/2 using simulated and measured channel data," *Electronics Letters*, vol. 37, No. 18, pp. 1137-1139, Aug. 2001.
- [8] Y. Xin, Z. Wang, and G. B. Giannakis, "Space-time constellation-rotating codes maximizing diversity and coding gains," in *Proc. of GLOBECOM Conf.*, San Antonio, TX, Nov. 25-29, 2001, pp. 455-459.
- [9] Y. Xin, G. B. Giannakis, and S. Zhou, "High-rate space-time layered multi-carrier and single-carrier transmissions over frequency-selective channels," *IEEE Trans. on Communications*, 2002 (submitted).